Composites: Part A 140 (2021) 106140

Contents lists available at ScienceDirect

Composites Part A

journal homepage: www.elsevier.com/locate/compositesa

Tensile-strength-controlling factors in unidirectional carbon fiber reinforced plastic composites

Go Yamamoto [a,b,*], Keita Koizumi [a], Takahiro Nakamura [a], Noriyuki Hirano [c], Tomonaga Okabe [a,d]

[a] Department of Aerospace Engineering, Tohoku University, 6-6-01 Aramaki-Aza-Aoba, Aoba-ku, Sendai 980-8579, Japan
[b] School of Mechanical Engineering, Sungkyunkwan University, Suwon 16419, Republic of Korea
[c] Composite Material Research Laboratories (CMRL), Toray Industries, Inc., 1515, Tsutsui, Masaki-cho, Iyogun, Ehime 791-3193, Japan
[d] Department of Material Science, University of Washington, Seattle, WA 98195, USA

A R T I C L E I N F O

Keywords:
A. Polymer-matrix composites (PMCs)
B. Mechanical properties
B. Stress concentrations
Crack tip opening displacement (CTOD)

A B S T R A C T

Factors governing the tensile strength of unidirectional carbon fiber reinforced plastic (CFRP) composites were experimentally investigated by focusing on the mechanical characteristics of the epoxy matrix. Correlation analysis was conducted to reveal the mechanical characteristics of the matrix that affect the surface stress concentration of an intact fiber caused by a fracture site in an adjacent fiber. The stress concentration factors (SCFs) were evaluated by implementing double-fiber fragmentation tests in conjunction with spring element model simulations. From investigating six types of epoxy materials, a reasonable correlation was observed between the matrix crack tip opening displacement (CTOD) and the SCF; the SCF increased approximately linearly with increasing CTOD. The results reported here suggest that CTOD is one of the important tensile-strength-controlling factors to consider for the development of stronger CFRP composites.

1. Introduction

Carbon fiber reinforced plastics (CFRPs) are applied for many engineering applications due to their high strength (stiffness)-to-weight ratio and tailorable mechanical properties. Consequently, further enhancement of the mechanical characteristics continues to be central to CFRP composite research. The tensile failure of CFRPs is known to be triggered by fiber fracture sequences within 0° plies. The individual fiber fractures that occur are now known to be induced by stress concentration generated on the intact fiber surface adjacent to the fiber break point [1]. Techniques such as Raman spectroscopy [2–3], synchrotron radiation computed tomography [4,5], and polarized light microscopy [6,7] have been employed to investigate the origin of stress concentration in addition to understanding fiber breaking processes. Recently, we conducted fundamental research to investigate the stress concentration factor (SCF) by performing multi-fiber fragmentation tests, subsequently comparing the experimental results to the corresponding spring element model simulation, which considers the added concentrated stress on the fiber surface adjacent to a broken fiber [7]. We reported that the degree of concentrated stress can be changed by modifying the mechanical properties of the epoxy matrix. Furthermore, even if the mechanical properties of the matrix vary, the predictive method can provide a reasonable prediction of the tensile strength of the unidirectional CFRP composites [7]. However, at that time, we could not provide a full explanation regarding why the tensile strength of the unidirectional CFRP composite varies depending on the mechanical characteristics of the matrix. Herein we conducted correlation analysis to reveal the mechanical characteristics of the matrix that affect the surface stress concentration of an intact fiber caused by the fracture site of an adjacent fiber. A scenario to explain the origin of stress concentration is proposed, based on experimental evidence and conclusions drawn from correlation analysis to investigate the relationship between possible influential factors and SCFs.

* Corresponding author at: Department of Aerospace Engineering, Tohoku University, 6-6-01 Aramaki-Aza-Aoba, Aoba-ku, Sendai 980-8579, Japan.
E-mail addresses: gyamamoto@tohoku.ac.jp (G. Yamamoto), koizumi@plum.mech.tohoku.ac.jp (K. Koizumi), takahiro.nakamura.s1@dc.tohoku.ac.jp (T. Nakamura), noriyuki.hirano.r7@mail.toray (N. Hirano), tomonaga.okabe.a8@tohoku.ac.jp (T. Okabe).

https://doi.org/10.1016/j.compositesa.2020.106140
Received 24 March 2020; Received in revised form 23 September 2020; Accepted 27 September 2020
Available online 16 October 2020
1359-835X/

2. Experimental and analytical procedures

2.1. Sample preparation and mechanical characterization

Epoxy specimens were prepared and their mechanical properties were measured to reveal the mechanical properties of the epoxy materials that affect the SCF. Among the six types of epoxy specimens investigated in this study, two specimens were synthesized using diglycidyl ether of bisphenol A (DGEBA) as the main agent and two curing agents (diethylenetriamine (DETA) and 4,4′-diaminodiphenyl sulfone (44DDS)). The other four specimens were provided by Toray Industries, Inc., Japan; they are hereafter referred to as "A-epoxy,“ "B-epoxy," "C-epoxy,“ and "D-epoxy," with the order of the names indicating the magnitude of their Young's moduli (i.e., the Young's modulus of the A-epoxy is the lowest). The mechanical properties of the epoxy materials were determined with uniaxial tensile loading and single-edge notched beam (SENB) tests. Schematics of the specimen configurations and experimental setups are shown in Fig. 1 (further details related to specimen preparation and mechanical evaluation can be found in the Supplementary Material).

Previously, we investigated how the SCF changes upon variation of both the number of fibers (2–4 fibers) and the interfiber spacing (3.5–20.0 μm) using multi-fiber fragmentation tests [7], although no apparent difference in the SCFs was observed under these conditions. Based on the above knowledge, the double-fiber fragmentation technique is employed in the current study to assess the SCFs. A high-strength, polyacrylonitrile (PAN)-based carbon fiber (TORAYCA™ T1100G) was used to fabricate the double-fiber fragmentation composites; the detailed composite preparation procedures, SCF determination procedures, and analytical model preparation can be found in [7,8] and the Supplementary Material.

2.2. Model preparation and determination of the stress concentration factor

The SCF (α) on the surface of an intact fiber was determined by employing the spring element model to investigate the SCF value, with the aim of ensuring that it was equivalent to the percentage of the coordinated fracture, which is defined as a failure occurring at the elements neighboring a broken element in the horizontal plane of the broken fiber element, as determined via double-fiber fragmentation testing. The details of model preparation, simulation procedures, and material properties can be found in the Supplementary Material. Herein, we considered the model in which the cross-section of the fiber divided into six segments, assuming the hexagonal fiber arrangement, as illustrated in Fig. 2(a). The surface SCF of the *i*-th fiber segment adjacent to a broken fiber at the plane of fracture was determined by assuming that it was α_i times the average stress (σ_f) on the surface of an adjacent fiber, which is expressed as follows:

$$\alpha_i = 1 + \gamma_i \left(1 - \frac{D_s}{l_s}\right), \quad (1)$$

where α_i is the SCF of a fiber adjacent to a broken fiber in the same plane; γ_i is the intensity attenuation factor, which is 0 for a fiber segment facing a neighboring intact fiber and $\alpha - 1$ for a fiber segment facing a neighboring broken fiber; D_s is the distance from the break point; and l_s is the stress recovery length. In the spring element model used in this study, the two longitudinal spring elements in the center of the model were assigned to the fibers and the remaining elements were assigned to the matrix. Thus, the matrix stiffness was implemented in the longitudinal spring elements. In our previous work, the stress gradient in an intact fiber was investigated using the three-dimensional finite element method [7]. Hence, the additional stress concentration was added in an ad-hoc manner to capture the experimentally measured correlations in the fiber breaks.

The strength of the *n*-th fiber segment is determined by choosing a random number ranging from 0 to 1 and solving the equation such that the fiber breakage probability equals a random number. The longitudinal element was removed from the model when the stress applied to a fiber at the *n*-th fiber segment achieved the statistical distribution of the strength of the fiber. A coordinated fracture was defined as a failure that occurred at neighboring elements next to a broken element in the same horizontal plane with respect to the broken fiber element, as illustrated in Fig. 2(b). Note that we previously confirmed that employing the above-mentioned procedures yields the predicted strengths of unidirectional CFRP composites that are reasonably consistent with the experimental data, irrespective of the differences in the mechanical characteristics of the matrix[7].

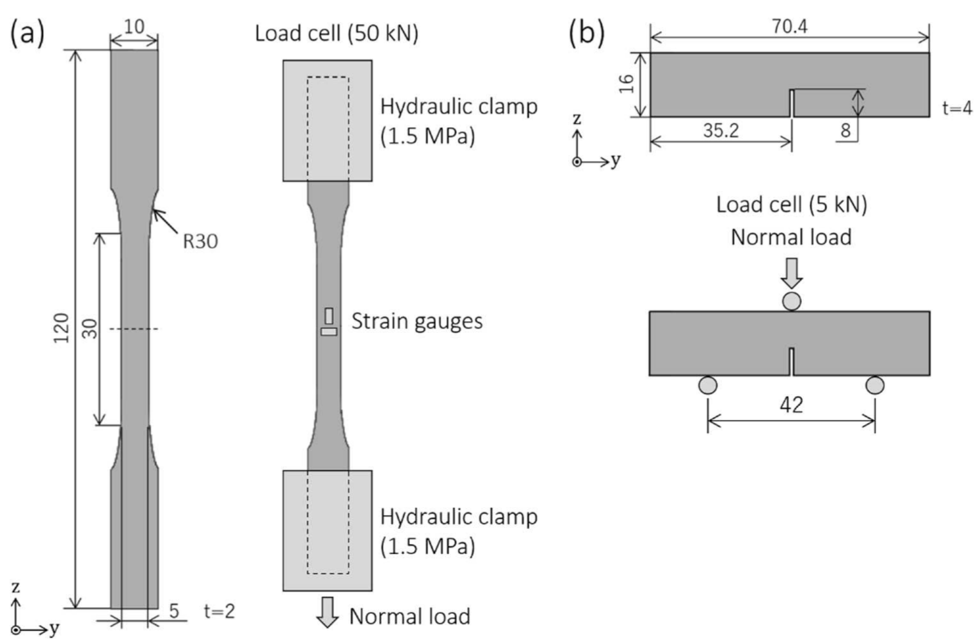

Fig. 1. Schematics of the specimen configurations and experimental setups for the (a) tensile-loading test and (b) single-edge notched beam test.

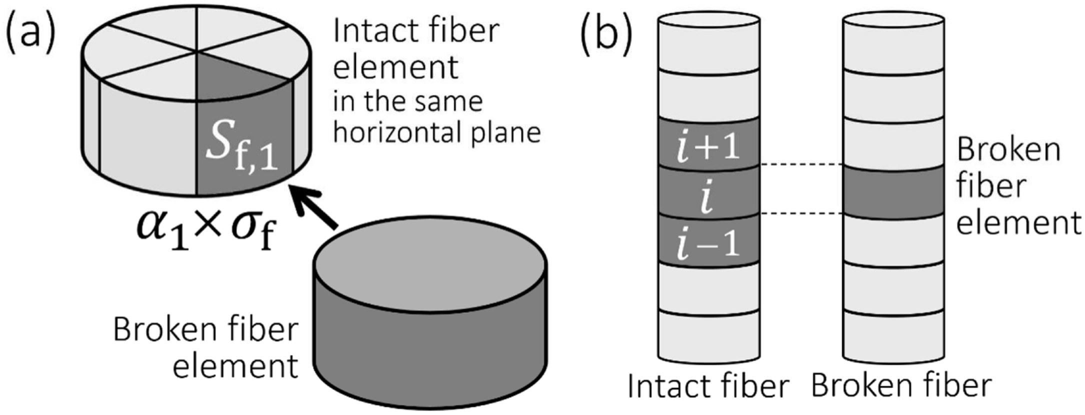

Fig. 2. Illustrations to (a) define the stress concentration on the surface of the (b) *i*-th fiber segment.

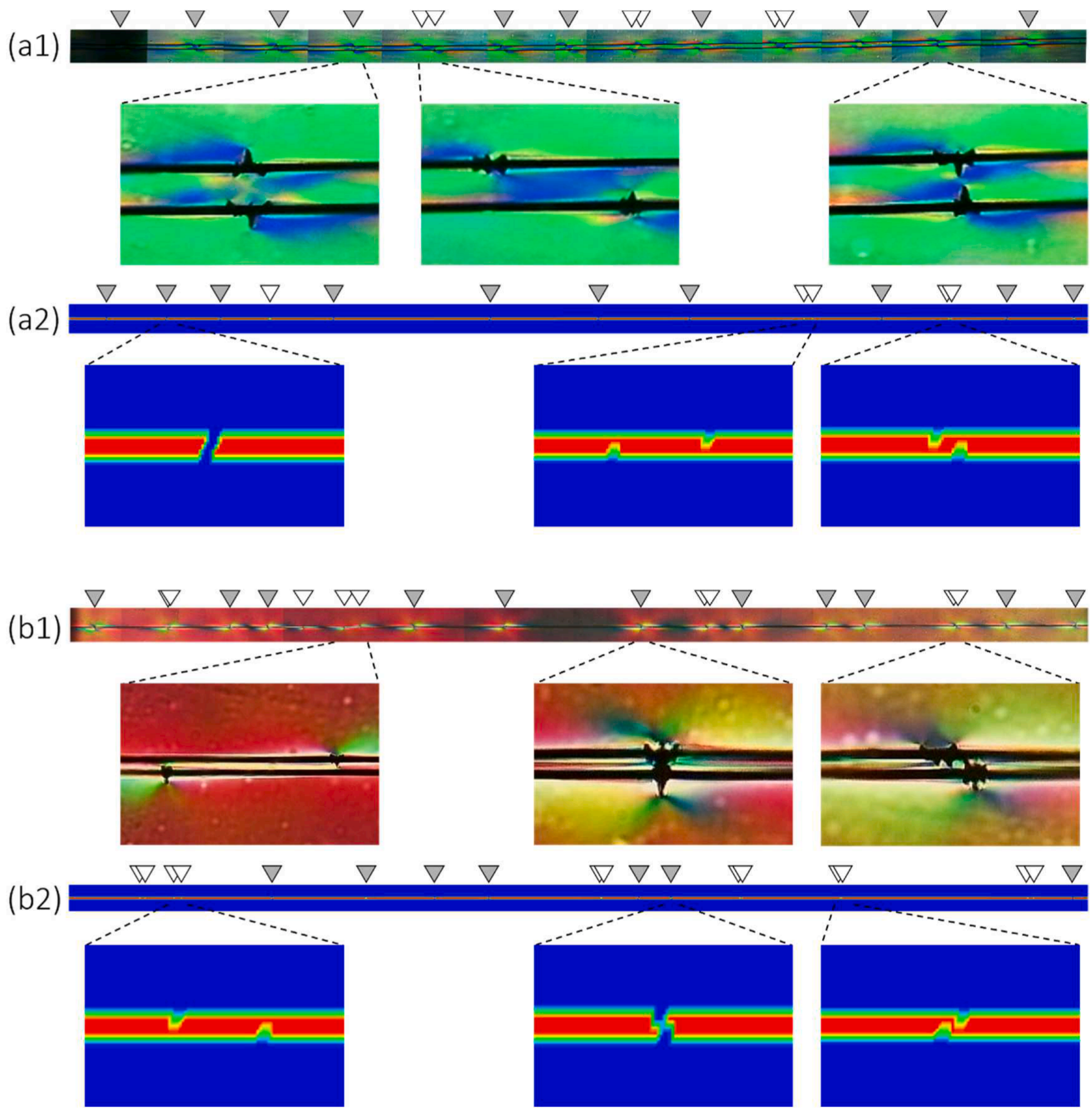

Fig. 3. Birefringence patterns in the double-fiber fragmentation composites prepared with DGEBA/44DDS (a1) and B-epoxy (b1). The corresponding simulation results are shown in (a2) and (b2). The symbols at the top of each fiber break point indicate the two types of fiber break; the filled symbol denotes coordinated fracture, while the open symbol indicates other fracture. (For interpretation of the references to colour in this figure legend, the reader is referred to the web version of this article.)

3. Results and discussion

All epoxy materials tested in the tensile loading experiments exhibited elasto-plastic behavior that is typically observed in conventional epoxy materials. The SENB specimens experienced catastrophic failure after reaching a maximum load and no nonlinear behavior was observed for all epoxy materials (Fig. S2). The mechanical properties of all the six epoxy materials are listed in Table S2 in the Supplementary Material.

The fiber fracture behavior of the double-fiber fragmentation composites was investigated to quantitatively determine the surface SCFs. This investigation revealed that matrix cracking and the coordination of fractures in adjacent fibers occur, regardless of the types of epoxy material. For example, Fig. 3 shows the birefringence pattern images at the fiber break points in the double-fiber fragmentation composites prepared with DGEBA/44DDS and B-epoxy. The corresponding two simulation results are shown in Fig. 3 (note that the images of the simulation results were processed to make the positional dependency of the fiber break points easier to understand, and they do not represent the actual stress distribution obtained from the simulations). The images were acquired at 3.26% fiber strain for DGEBA/44DDS and at 3.10% fiber strain for B-epoxy. The symbols at the top of each fiber break point indicate the two types of fiber break. The filled symbols denote the coordinated fracture defined based on the nature of elasto-plastic polymer material fracture phenomena [9], while the open symbols indicate the other phenomena. As a fiber–fiber interaction criterion, fiber fractures that occur at an angle between 0° and 45° are defined as coordinated fractures. It can be observed from Fig. 3(a1) and 3(b1) that the matrix cracks propagated from the fiber break points, and a large number of fiber failures occured at similar positions, indicating that the stress concentration caused by fiber fracture was sufficiently high to cause the adjacent fiber to fracture. A similar observation was made from simulation results shown in Fig. 3(a2) and (b2). The percentages of coordinated fracture (and standard deviation) obtained by the experimental and simulated results for DGEBA/44DDS were 75.7% (±10.3%) and 76.3% (±12.8%), respectively. The corresponding values for B-epoxy were 48.3% (±14.1%) and 46.5% (±15.9%). The experimentally obtained percentages of coordinated fracture (and standard deviation) for the DGEBA/DETA, A-epoxy, C-epoxy, and D-epoxy composites were 89.3% (±9.9%), 43.2% (±14.5%), 54.4% (±15.5%), and 9.1% (±4.3%), respectively. Note that in our previous study, we prepared fiber fragmentation composites in which two T1100G carbon fibers were embedded in B-epoxy material, and then carried out fragmentation tests under the same conditions as those used in this study. The interfiber spacing in the composites was approximately 200 µm. Thus interfiber spacing is equivalent to the diameter of approximately 40 fibers and is unaffected by the fracture of the counterpart fiber[10]. The percentages of coordinated fracture in the composites was measured using the processed images so that the interfiber spacing was 10 µm (the average interfiber spacing in the study). Consequently, the percentage of coordinated fracture measured to be 7.7%. This value is close to that observed for the composite prepared with D-epoxy, suggesting that the fiber failure process in D-epoxy matrix composites is predominantly governed by the statistical strength distribution of the fibers.

Quantitative determination of the SCFs on the surface of intact fibers was achieved by implementing the spring element model (Supplementary Figs. S3a–S3f). For example, for DGEBA/44DDS, the SCF on the surface of an intact fiber was determined to be 2.16 upon comparing the simulated percentages of coordinated fractures to the corresponding experimental observations, indicating that for composites fabricated with DGEBA/44DDS, the concentrated stress acting on the fiber surface is approximately twice that of the fiber stress with no additional surface stress concentration. The percentages of coordinated fracture, applied fiber strain, and SCFs for the six composites are listed in Table S3 in the Supplementary Material.

In order to reveal the mechanical characteristics of the epoxy materials that influence the stress concentration generated on an intact fiber surface, the correlation between the SCF and mechanical properties of the epoxy materials was analyzed. The relationships of SCF with the tensile strength, Young's modulus, fracture toughness, crack tip opening displacement (CTOD), and plastic zone size of the matrix materials are shown in Fig. 4(a)–(e), respectively. The dashed lines in Fig. 4 indicate the regression lines calculated by the least-squares method, assuming a linear relationship between the SCF and the five properties of the matrix materials. Although some variation occurs, the epoxy materials with both higher tensile strength and Young's modulus generally exhibit lower SCFs, while those with higher fracture toughness lead to higher SCFs. This implies that epoxy materials with brittle-like characteristics are effective for decreasing the SCF, whereas those with ductile-like characteristics lead to an increase in the SCF. The highest correlation relationship was observed for the tensile strength with the coefficient of determination (R^2 value) of 0.85. The R^2 values for the Young's modulus, fracture toughness, CTOD, and plastic zone size were 0.76, 0.55, 0.80, and 0.70, respectively. Even though the highest correlation was observed for the tensile strength, it represented the macroscopic mechanical characteristics of the materials. Thus, we expect that CTOD (and plastic zone size) seems to make sense as a measure that represents the fracture phenomenon of fibers under the stress field around the crack tip. The high SCF observed for the ductile-like epoxy materials can be attributed to the large crack opening around the crack tip.

CTOD, defined as the displacement transverse to the crack tip, appears to impact the SCFs. The generalized equation describing CTOD (δ) is expressed as follows [11]:

$$\delta = \frac{K_{\mathrm{Ic}}^2}{E\sigma_{\mathrm{y}}}, \tag{2}$$

where K_{Ic} is the mode I fracture toughness, E is the Young's modulus, and σ_{y} is the yielding stress. Following ASTM recommendations [11], the CTOD was calculated by substituting the yielding stress (σ_{y}) with tensile strength (σ) in Eq. (2). As shown in Fig. 4(d), a positive linear correlation exists between the CTOD and SCF; an epoxy material with a larger CTOD tends to exhibit a higher SCF. Furthermore, the epoxy materials with ductile-like characteristics possessed a large plastic zone, whose size increased with an increase in the SCF (Fig. 4(e)). This trend is similar to that observed for the CTOD.

The size of the plastic zone ahead of a crack tip under plane strain conditions (r_{p}) is expressed as follows:

$$r_{\mathrm{p}} = \frac{1}{4\sqrt{2}\pi}\left(\frac{K_{\mathrm{Ic}}}{\sigma_{\mathrm{y}}}\right)^2. \tag{3}$$

Eq. (3) can therefore be used to assess differences in the extent of stress concentration generated on intact fiber surfaces. As mentioned earlier, the matrix crack around the original broken fiber is expected to be one cause of additional stress concentration [7]. The matrix crack caused by fiber breakage propagates toward the rigid intact fiber, resulting in stable crack growth. This crack remains without reaching the fiber/matrix interface after approaching the intact fiber.

Additional stress can continue to be applied to epoxy materials with large CTOD until the opening reaches a critical value because of the high stress concentration in the process zone. On the other hand, epoxy materials with small CTOD alleviate the additional stress concentration. These are considered to be the possible mechanism by which CTOD affects the additional stress concentration.

4. Conclusions

We have reported an experimental study in which we investigated the tensile strength-controlling factors of unidirectional CFRP composites, focusing on assessing the mechanical characteristics of the epoxy matrix. The degree of concentrated stress acting on the intact fiber surface, which determines the tensile strength properties of

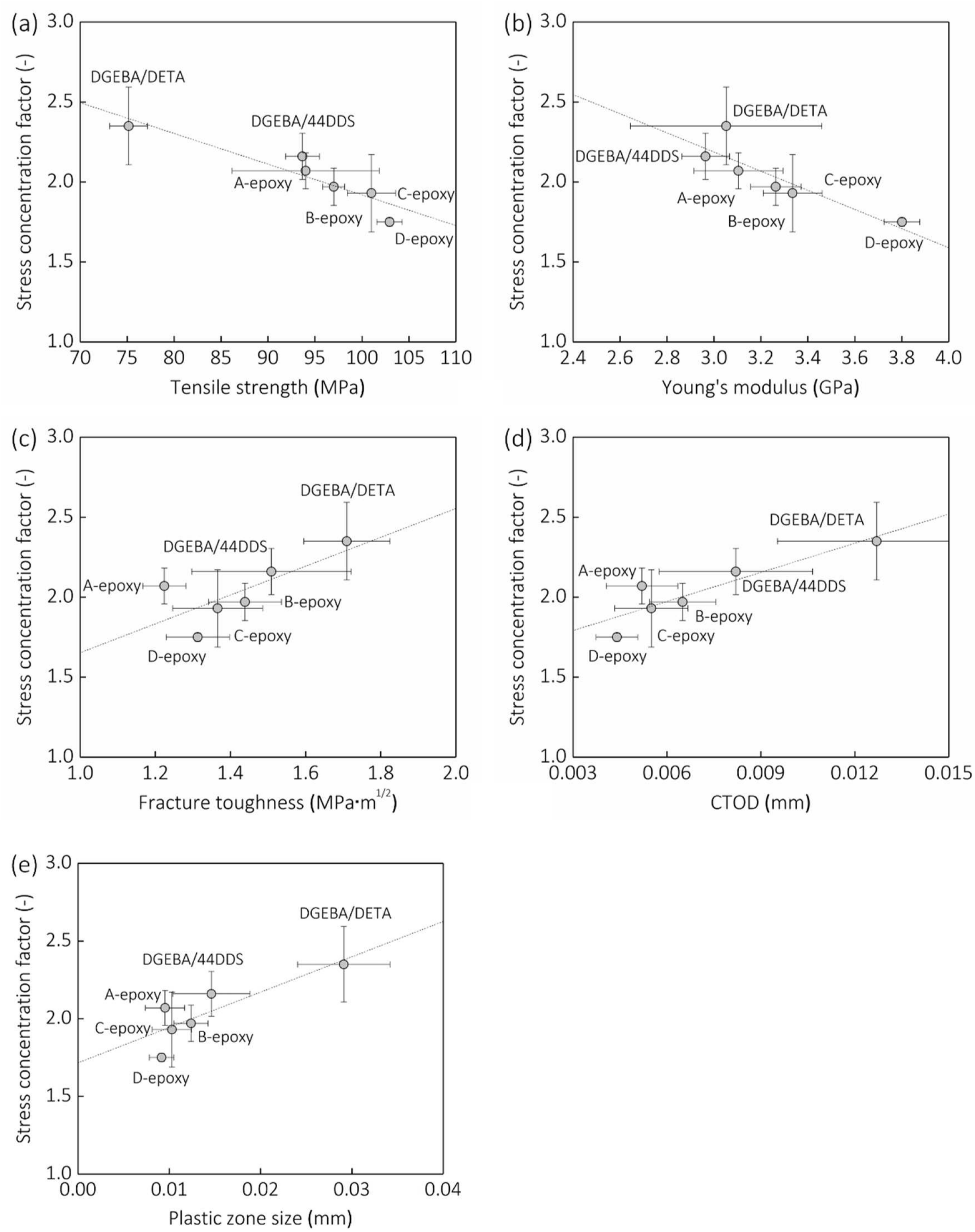

Fig. 4. Relationship of the stress concentration factor with (a) tensile strength, (b) Young's modulus, (c) fracture toughness, (d) crack tip opening displacement (CTOD), and (e) plastic zone size. The dashed lines indicate the regression lines calculated by the least-squares method, assuming a linear relationship between the SCF and five properties of the matrix materials.

unidirectional CFRP composites, was evaluated by implementing double-fiber fragmentation tests in conjunction with spring element model simulations. Correlation analysis was conducted, with the aim of extracting the factors that characterize the tensile strength of the unidirectional CFRP composites. The analysis of six epoxy materials with different mechanical characteristics revealed that the matrix crack tip opening displacement (CTOD), which is characterized by the tensile strength, Young's modulus, and mode I fracture toughness, exhibited a linear correlation with the surface SCF, with the SCF increasing from 1.75 to 2.35 with an increase CTOD. These results revealed that CTOD is one of the dominant factors influencing the tensile strength characteristics of unidirectional CFRP composites. Ultimately, our results provide a fundamental framework for guiding the creation of high-performance CFRP composites for epoxy matrices.

CRediT authorship contribution statement

Go Yamamoto: Conceptualization, Data curation, Formal analysis, Funding acquisition, Investigation, Project administration, Supervision, Validation, Visualization, Writing - original draft, Writing - review &

editing. **Keita Koizumi:** Data curation, Investigation, Visualization. **Takahiro Nakamura:** Investigation. **Noriyuki Hirano:** Project administration, Resources. **Tomonaga Okabe:** Conceptualization, Formal analysis, Funding acquisition, Methodology, Project administration, Software, Supervision, Validation, Writing - review & editing.

Declaration of Competing Interest

None.

Acknowledgements

The authors thank Prof. T. Hashida and Mr. T. Suzuki of the Fracture and Reliability Research Institute, Tohoku University, for technical assistance in the fracture toughness measurements. This work was partly supported by Toray Industries, Inc., the Council for Science, Technology and Innovation (CSTI), Cross-ministerial Strategic Innovation Promotion Program (SIP), and JSPS KAKENHI [grant number 18K04721]. We would like to thank Editage for English language editing.

Appendix A. Supplementary material

Supplementary data to this article can be found online at https://doi.org/10.1016/j.compositesa.2020.106140.

References

[1] Hedgepeth JM, Van Dyke P. Local stress concentrations in imperfect filamentary composite materials. J Compos Mater 1967;1(3):294–309.
[2] van den Heuvel PWJ, Peijs T, Young RJ. Failure phenomena in two-dimensional multi-fibre microcomposites: 2. A Raman spectroscopic study of the influence of inter-fibre spacing on stress concentrations. Compos Sci Technol 1997;57(8):899–911.
[3] van den Heuvel PWJ, Peijs T, Young RJ. Failure phenomena in two-dimensional multi-fibre microcomposites. Part 4: A Raman spectroscopic study on the influence of the matrix yield stress on stress concentrations. Compos A 2000;31(2):165–71.
[4] Scott AE, Mavrogordato M, Wright P, Sinclair I, Spearing SM. In situ fibre fracture measurement in carbon-epoxy laminates using high resolution computed tomography. Compos Sci Technol 2011;71(12):1471–7.
[5] Swolfs Y, Morton H, Scott AE, Gorbatikh L, Reed PAS, Sinclair I, et al. Synchrotron radiation computed tomography for experimental validation of a tensile strength model for unidirectional fibre-reinforced composites. Compos A 2015;77:106–13.
[6] Watanabe J, Tanaka F, Higuchi R, Matsutani H, Okuda H, Okabe T. A study of stress concentrations around fiber breaks in unidirectional CF/epoxy composites using double-fiber fragmentation tests. Adv Compos Mater 2018;27(6):575–87.
[7] Yamamoto G, Onodera M, Koizumi K, Watanabe J, Okuda H, Tanaka F, Okabe T. Considering the stress concentration of fiber surfaces in the prediction of the tensile strength of unidirectional carbon fiber-reinforced plastic composites. Compos A 2019;121:499–509.
[8] Okabe T, Sekine H, Ishii K, Nishikawa M, Takeda N. Numerical method for failure simulation of unidirectional fiber-reinforced composites with spring element model. Compos Sci Technol 2005;65(6):921–33.
[9] Huang H, Talreja R. Numerical simulation of matrix micro-cracking in short fiber reinforced polymer composites: Initiation and propagation. Compos Sci Technol 2006;66(15):2743–57.
[10] Van Den Heuvel PWJ, Van Der Bruggen YJW, Peijs T. Failure phenomena in multifibre model composites: Part 1. An experimental investigation into the influence of fibre spacing and fibre-matrix adhesion. Compos A 1996;27(9):855–9.
[11] ASTM D5045-99: Standard test methods for plane-strain fracture toughness and strain energy release rate of plastic materials; 1999.